

Eruption of the magnetic flux rope in a fast decayed active region

Shangbin Yang*

Key Laboratory of Solar Activity, National Astronomical Observatories, Chinese Academy of Sciences, Beijing 100012, China

Wenbin Xie

Jilin Normal University, 136000 Siping, Jilin Province, China

Jihong Liu

Shijiazhuang University, 050035 Shijiazhuang, Hebei Province, China

Abstract

An isolated and fast decayed active region (NOAA 9729) was observed when passing through solar disk. There is only one CME related with it that give us a good opportunity to investigate the whole process of the CME. Filament in this active region rises up rapidly and then hesitates and disintegrates into flare loops. The rising filament from EIT images separates into two parts just before eruption. A new filament reforms several hours later after CME and the axis of this new one rotates clockwise about 22° comparing with that of the former one. We also observed a bright transient J-shaped X-ray sigmoid immediately appears after filament eruption. It quickly develops into a soft X-ray cusp and rises up firstly then drops down. Two magnetic cancelation regions have been observed clearly just before filament eruption. Moreover, the magnetic flux rope erupted as the magnetic helicity approach the maximum and the normalized helicity is -0.036 when the magnetic flux rope erupted, which is close to the prediction value of [Zhang et al. \(2008\)](#) based on the theoretical non-linear force-free model.

Keywords: Sun; Magnetic helicity; CMEs; filament eruption

*Corresponding author

Email address: yangshb@bao.ac.cn (Shangbin Yang)

1. Introduction

Coronal mass ejections (CMEs) have been one of the outstanding problems of solar physics. The nature of driver and initiation mechanism for the sudden explosive release of the stored free magnetic energy are still unclear. It is proposed that CMEs are that metastable magnetic configurations are followed by some finite perturbation or some additional energy build-up and make a eventual catastrophic transition to a lower energy state or to non-equilibrium state (Ref. [Priest & Forbes, 2002](#); [Lin et al., 2003](#)). There are already several mechanisms to cause the catastrophic transition have been proposed such as slow reduction of the overlying flux ([Forbes & Priest, 1995](#); [Priest & Forbes, 1990](#)), photospheric converging and shear motions ([Forbes et al., 1994](#); [Antiochos et al., 1994](#)), flux emergence ([Feynman & Martin, 1995](#)), etc.

As a candidate for the metastable configuration, [Sturrock et al. \(2001\)](#) considered a long twisted flux tube, anchored at both ends in the photosphere with overlying magnetic arcade. They argue from a simple order-of-magnitude calculation that part of the flux tube will open up to infinity if there are 1-2 full winds for each field line in the flux tube even this configuration is stable according to linear MHD stability theory. [Fan \(2005\)](#) carried out simulations in a spherical geometry of the evolution of coronal magnetic field as an a twisted magnetic flux rope emerges slowly into a preexisting coronal potential arcade field. She find that the flux tube becomes kinked and ruptures through the arcade field and cause a eruption when the twist in the emerged tube reaches a critical amount. [Török & Kliem \(2005\)](#) use the flux rope model of [Titov & Démoulin \(1999\)](#) as the initial condition to get a simulation which have a good agreement with the development of helical shape and the rise profile of a failed filament eruption described by [Ji et al. \(2003\)](#). Kinking movement in the eruption of filament are also usually observed ([Liu et al., 2007, 2008](#)). In addition, soft X-ray images of solar active regions frequently show S- or inverse-S (sigmoidal) morphology. [Canfield et al. \(1999\)](#) found that active regions containing X-ray sigmoids are more likely to erupt and many eruption also associated with sigmoid structure. While the question of whether there exit highly twisted flux ropes with more than one wind between anchored ends susceptible to the kink instability as precursors for eruptive flux tube remains a topic of debate (e.g. [Rust & Kumar,](#)

1996; Leamon et al., 2003; Leka et al., 2005; Rust & LaBonte, 2005) when these authors investigate the relation between the shape of X-ray sigmoid and eruption.

Gibson & Fan (2006) demonstrated the partial expulsion of a three dimensional magnetic flux rope erupts when enough twist has emerged to induce a loss of equilibrium. After multiple reconnections at current sheets that form during the eruption, the rope breaks in two, so that only a part of it escapes. The "degree of emergence" of a pre-eruption flux rope, whether it possess bald-patch (BP) or whether it is high enough in the coronal to possess an X-line determines whether the rope is expelled totally or partially. Their simulation result is well consistent with the partial eruption model described by Gilbert et al. (2001). But should a twisted or kinked or magnetic flux tube need kink instability or twist over such threshold to eruption? Is it kink instability or kink-induced instability in a filament eruption (Gilbert et al., 2007)? For example, the kink instability may be occurring in conjunction with a breakout scenario (Williams et al., 2005). Low (2001) also argued that a force-free magnetic field in the unbounded space outside a sphere cannot be in equilibrium if the amount of detached flux is too large compared to the amount of anchored flux. Eruption of magnetic flux tube can also be caused by another instabilities such as torus instability (Kliem & Török, 2006) and Ballooning instability (e.g. Fong et al., 2001). So it is essential to investigate the whole eruptive process of a magnetic flux tube since emergence and evolution of structure in different wavelength especially the soft X-ray sigmoid for study how the metastable state is established and how to loss equilibrium and erupt for this magnetic flux tube.

On the other hand, Zhang et al. (2006) pointed out that the accumulation of magnetic helicity in the corona plays a significant role in storing magnetic energy. They propose a conjecture that there is an upper bound on the total magnetic helicity that a force-free field can contain. The accumulation of magnetic helicity in excess of this upper bound would initiate a non-equilibrium situation, resulting in a CME expulsion as a natural product of coronal evolution. Berger and Field (1984) proposed the concept of relative magnetic helicity and the formula to get the accumulated magnetic helicity across a surface into a volume from the movement in that surface. Chae et al. (2001) firstly calculated the accumulated magnetic helicity by applying LCT (Local Correlation Tracking) to MDI data. However, the relation between accumulated magnetic helicity and eruption of magnetic flux tube has not been checked in the past work. What is the accumulated helicity for

a emerging flux tube when it erupts? We need to investigate the process of magnetic helicity accumulation in an eruption.

NOAA 9729 is an active region emerging on Dec. 05, 2001. Its initial tilt angle is almost perpendicular to the equator of sun and then develop to a bipolar active region. It rapidly dispersed in the following days and disappeared on Dec. 08, 2001 from white light (WL) image. The evolution of such photospheric concentrations are usually been explained in terms of the rising of very distorted flux tubes. [Weart \(1970, 1972\)](#) also noticed the almost random distribution of the starting tilt of emerging bipoles, which subsequently became more parallel to the equator, and proposed that this was caused by the emergence of twisted flux tubes. Especially, a kinked flux tube arches upward and evolves into a buckled loop with a local change of tube orientation at the loop apex that exceeds 90 degrees from the original direction of the tube [Fan et al. \(1999\)](#). The characteristic of this emerging active region implies that there are strong twist in it. Moreover, there is only one CME related with it since emergence. This give us a good opportunity to investigate the whole process of a CME for a strong twisted flux tube.

In this paper we use multiple wavelengths and instruments to investigate the whole CME process. We also calculate the accumulated magnetic helicity since this active region emerged. We give a quick survey of the instrument and data sets used in this study (Sec. 2.1). We describe the evolution of white light and emerging speed in Sec. 2.2. we describe the evolution of H-alpha, EIT, X-ray, and corresponding CMEs from Sec. 2.3 to 2.6. We calculate accumulated magnetic helicity in Sec. 2.7. The summary and discussion is represented in Sec. 3.

2. OBSERVATIONS AND DATA ANALYSIS

2.1. Instrumentation and Data

We use data of SOHO/MDI to investigate the evolution of White light image and line-of-sight magnetograms ([Scherrer et al., 1995](#)). We use data of high-resolution global $H\alpha$ network to investigate the evolution of Chromosphere. We use data of Extreme Ultraviolet Imaging Telescope to investigate the evolution of low Corona (EIT; [Delaboudinière et al., 1995](#)). We use soft X-ray images obtained with the Soft X-ray Telescope (SXT) on board the Yohkoh satellite to investigate the evolution of high Corona ([Tsuneta et al., 1991](#)). We use Large Angle Spectrometric Coronagraph (LASCO; [Brueck-](#)

ner et al., 1995) aboard SOHO to investigate the CME associated with this active region.

2.2. Estimation of emerging speed

NOAA 09729 emerged from the convective zone at about 03:26UT on December 05, 2001 seen from WL image. It developed to a bipolar active region rapidly and disappeared on Dec. 08, 2001. The evolution of tilt angle and the distance between two polarities considering the barycenters of the leading and following polarities are shown in Fig. 1. Its initial title angle is almost perpendicular to the equator of sun and still disobeyed Joy's law when this active region disappeared despite the connecting line between two polarities became more parallel to the equator. The maximum distance (d_{max}) between two polarities is at 07:06UT on December 7. If we suppose the coronal part of one active region is represented by a single semicircular loop. The initial distance (d_{min}) will be the chord of the semicircle and the maximum distance (d_{max}) will be the diameter of this semicircle. The emerging height in this time interval is approximately $\sqrt{(d_{max}^2 - d_{min}^2)/4} = 30.6Mm$ under this assumption and the corresponding average emerging speed is about 0.164km/s. The mean magnetic field in this active region is about 100 Gauss and the corresponding Alfvén speed at photosphere is about 8.9Km/s . The emerging speed will be about 0.018 of local V_A . Fig. 2 shows the time sequence of WL images.

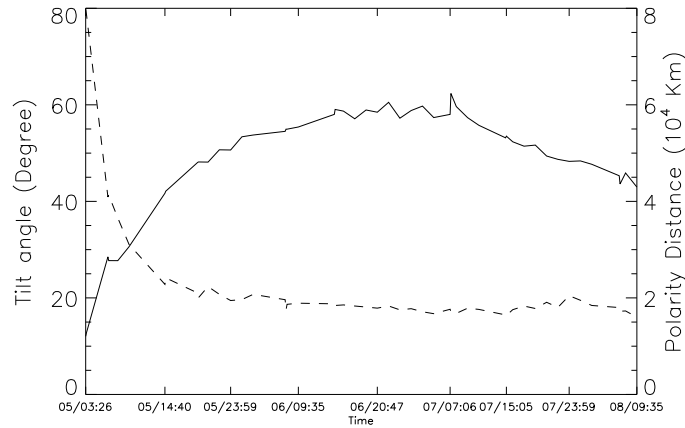


Figure 1: Evolution of tilt angle (dashed line) and distance (solid line) between two polarities.

2.3. $H\alpha$ Evolution

Fig. 3 shows the evolution of NOAA 9729 in $H\alpha$. Top two rows (Fig. 3a-f) show the evolution of $H\alpha$ from December 05 to 09, 2001. The filament in this active region didn't appeared before 22:30 UT December 4. At 16:59UT on December 5, a inverse-S shaped filament has appeared in the $H\alpha$ locating above polarity inversion line (PIL) which is shown in Fig. 3b. The shape of this filament didn't changed a lot after this moment while the middle channel of this filament labeled by red solid line in Fig. 3c separated into several parts and is not clear than the initial one on December 5. The filament still existed after eruption at about 02:34UT on December 7 and there is an obvious clockwise rotation of the middle channel of the filament. The clockwise rotation angle of the filament middle channel is approximately 22° denoted in the Fig. 3. The filament almost kept the same shape in the next two days after this active region disappeared from WL, which can be seen in the Fig. 3 (e-f).

Bottom two rows (Fig. 3g-n) show the evolution detail in $H\alpha$ when eruption occurred on December 07, 2001. There are two stages for the filament eruption. Firstly, the left part in the middle filament channel became thin and disappeared gradually from Fig. 3g-j. The left part of the middle filament channel has disappeared entirely at 01:45UT. The right part of the filament disappeared totally before 02:12UT in Fig. 3. One interesting phenomena is that the right part of filament became thicker before eruption which is different with the left one. At 03:41UT after eruption, two bright foot-points regions have appeared and the brightness decreased with time. The shape of the two bright regions is consistent with cancelation region of magnetic field region in Fig. 6f. The filament above the polarity inversion line (PIL) also gradually appeared again after the eruption, which is shown from Fig. 3l-n.

2.4. EIT evolution

Fig. 4 shows the detail evolution of NOAA 9729 EIT images in the 171 Å filter when the eruption occurred on December 7. The filament in EUV wavelength can be seen clearly from the Fig. 4. There are similar stages for the filament eruption from EUV comparing with that in $H\alpha$. Two square boxes in Fig. 4a denotes two EUV bright points. The left part risen up labeled by red arrow in Fig. 4b and it did not erupt immediately. In the same time, The upper EUV bright point disappeared. The right part of the filament risen up subsequently, which is labeled by blue arrows in Fig. 4b-c. In Fig. 4d, the risen filament separated in to two parts that labeled by two red

arrows. At 02:34UT on December 07, the filament eruption occurred. Fig. 4e shows the rising filament and a kinked-like structure can also be found. After eruption, two bright EUV regions formed on the two foot-points of this flux tube which is labeled by red boxes in Fig. 4f. At 03:10UT, a bright region denoted by red boxes above the inversion line also has formed subsequently and it expanded along the inversion line to the opposite directions and post-flare loops formed in the same time, which is shown from Fig. 4h-j. In the following several hours, the formed post-flare loop continued rising up and it became cooling gradually and disappeared at last from Fig. 4k-l.

2.5. *Yohkoh X-ray Evolution*

Fig. 5 shows the evolution of NOAA 9729 in soft xray. An Inverse S-shaped sigmoid structure formed clearly since December 05. Such inverse S-shaped sigmoid is an indication of the presence of negative twist in the magnetic field (Rust & Kumar 1996; Pevtsov et al. 2001). The negative chirality is the same as that deduced from the shape of filament in Fig. 3. The shape of this sigmoid didn't change a lot in the following days before eruption and it rotated clockwise which is consistent with the rotation sense of connecting line of the two foot-points from WL image as presented in Fig. 2. An X-ray bright point existed long time before eruption as labeled by the white square box in Fig. 5f-i. At about 00:51UT on December 7, the left part of the sigmoid risen up as denoted by the green arrow in Fig. 4m. The time is consistent with the eruption of left part of the filament in the $H\alpha$ images Fig. 3g-j and the EUV images Fig. 4b. At 02:29UT, the sigmoid has erupted and a transient J-shaped sigmoid formed at the same time. This transient J-shaped sigmoid existed earlier than the two bright EUV foot-points denoted by the two red square boxes in Fig. 4f and it became broad subsequently which can be seen from Fig. 4o. At 03:53UT on December 07 in Fig. 4p, a X-ray cusp has formed and it risen up firstly as labeled by white arrow in Fig. 4q. This cusp was diffused at last, which can be seen in Fig. 4r.

2.6. *CME evolution*

Eruption of this active region brought one partial halo CME which is recorded in CME catalog maintained at the CDAW Data Center. The first appearance in the LASCO/C2 field of view (FOV) is at 03:06UT on December 7 and the central position angle (CPA) is 343° . According to the description in this CME catalog list, the linear speed obtained by fitting a straight line to the height-time measurements is 803.2km/s. The acceleration of such CME

is $-51.01 m/s^2$. This CME slows down within the LASCO FOV while it has escaped out of ten solar radius. The eruptive part of the filament escaped successfully. The speed value and deceleration satisfy the character of the fast CMEs. Fast CMEs originate from an active region and their initial speeds are well above the CME median speed, 400 Km/s. They show no significant acceleration, but may show some deceleration (St. Cyr et al., 2000).

2.7. Evolution of magnetic field and helicity

Fig. 6 shows the evolution of line-of-sight magnetic field of this active region. Two magnetic cancellation regions along the PIL about four hours before flux tube eruption are labeled by red circles in fig.3e. After the eruption the two cancellation regions disappeared.

The accumulated magnetic helicity was calculated using full-disk line-of-sight magnetograms taken by SOHO/MDI. From the photospheric magnetic field observations the helicity flux across the photosphere \mathbf{S} can be calculated by

$$\frac{dH_R}{dt} = -2 \int (\vec{A}_p \cdot \vec{U}) B_n d\vec{S}, \quad (1)$$

where \vec{U} denotes the horizontal velocity field. The vector potential \vec{A}_p is obtained by applying Local Correlation Tracking (LCT) and Fast Fourier Transforms (FFT) to the normal components of the photospheric magnetic field B_n (Chae et al., 2001). After applying nonlinear mapping and flux density interpolation the geometrical foreshortening was corrected (Liu & Zhang, 2006; Yang et al., 2009b). To reduce the noise, we set the horizontal velocity to zero in regions where the magnetic field is small ($< 10G$). In order to better track the emerging regions and to exclude the effect of relative quiet regions outside the emergence sites, we set the horizontal velocity to zero in regions of a weak cross-correlation (< 0.9) of two magnetograms. We calculate the accumulated magnetic helicity as

$$H(t) = \int_0^t \frac{dH_R(t)}{dt} dt \quad (2)$$

where the starting moment of time $t=0$ corresponds to the beginning emergence of the active regions. Further, the following definition of the normalized magnetic helicity H_{norm} is used:

$$H_{norm}(t) = \frac{|H_m(t)|}{\Phi_m^2}, \quad (3)$$

where Φ_m is the maximum absolute value of the magnetic flux through the photosphere of the studied newly emerging AR.

Fig. 7 depicts the evolution of parameter that the total relative magnetic helicity normalized by one-half of the maximum sum of the unsigned positive and negative magnetic fluxes ϕ . This emerging flux tube take negative magnetic helicity to the corona. The flux tube in AR 9729 erupted at 02:34 UT on December 07. Just at this moment, this normalized parameter is -0.036. Recently, new methods have been used to calculate the horizontal motion of magnetic structures on the photosphere, in which the evolution of vertical magnetic fields satisfy the ideal induction equation (e.g. [Welsch et al., 2007](#)). The rotation motions of the magnetic features, is introduced to get a more precise measurement of the magnetic helicity ([Pariat et al., 2005](#); [Schmieder et al., 2011](#); [Romano et al., 2011](#)). The difference of magnetic helicity fluxes obtained from different methods is usually within 15% ([Romano et al., 2011](#)). The estimate the final normalized helicity is -0.036 ± 0.0054 when the magnetic flux tube erupted in AR 9729.

3. SUMMARY AND DISCUSSION

In this paper, we have presented a multiple wavelengths study of emergence of a fast decayed active region NOAA 9729 and associated eruption. Our main observation results are summarized as follows.

1. NOAA 9729 emerged from convective zone with initial tilt angle is almost perpendicular to the equator of sun. The connecting line between leading polarity and following polarity rotated clockwise. This active region still disobeyed Joy's law when it disappeared from WL.

2. The filament in $H\alpha$, EUV structure and sigmoid in X-ray all show the same inverse S-shape. This is a indication of negative helicity in the flux tube. The eruption stages in the three wavelength are also similar. The left part of the structure risen up and the right part risen subsequently. Then, the eruption occurred as the pre-eruption state evolved.

3. A filament in $H\alpha$ reformed again after eruption. The middle channel of filament in $H\alpha$ rotated clockwise about 22° than before.

4. EUV structure separated into two parts before eruption. The sudden rising flux tube in the eruption showed a kinked structure. The EUV bright regions disappeared after the flux tube risen up. The risen flux tube dropped down and flare loops formed. The intimal bright point formed above the PIL and expanded along the two opposite directions of this PIL.

5. Inverse S-shaped sigmoid structure became thinner before eruption. A transient J-shaped sigmoid structure formed subsequently after eruption just before EUV bright region formed above the PIL formed.

6. The associated CME recorded is a partial halo CME. The linear speed obtained by fitting a straight line to the height-time measurements is 803.2km/s. The acceleration of such CME is $-51.01m/s^2$. Associated CME in the eruption belongs to the fast CME.

7. From line-of-sight magnetic field, two magnetic cancelation regions just underneath filament can be found before eruption and these regions disappeared after eruption. Negative helicity was taken by the emergence of magnetic flux and differential rotation. The parameter that the total relative magnetic helicity normalized by one-half of the maximum sum of the unsigned positive and negative magnetic fluxes is -0.036 when eruption taken place.

What's the metastable structure before eruption? Firstly, we can deduced it as a negative twist flux tube. As described in the sum. 2, all structures in the emerging flux tube showed a inverse S-shaped structure. These type of structures are associated with negative twist magnetic flux tube. The negative accumulated magnetic helicity also implies existence of negative twist in the flux tube. Secondly, we can deduce this flux tube is a kinked flux tube. As the description in the sum. 1, this active region disobeyed Joy's law and the tilt angle rotated clockwise. If we consider this flux tube as a simple flux tube described in [Lopez Fuentes et al. \(2003\)](#), such type of flux tube should have a negative writhe (right hand) flux tube. In the framework of a kink instability model as simulated by [Fan et al. \(1999\)](#), also noted in [Leka et al. \(1996\)](#) and [Linton et al. \(1998\)](#), the sign of the writhe of kinked flux tubes would be the same as that of the twist within the tubes due to conservation of helicity. When a horizontal flux tube is emerging twisted right-handed (left-handed) of negative (positive) magnetic helicity, the writhe of the tube axis resulting from kink instability is also right-handed (left-handed). This would leads to a clockwise (counter-clockwise) rotation of the apex portion of the rising tube as viewed from the top. Such scenario well explains the evolution in sum. 1. ([Yang et al., 2009b](#)) also pointed out that the emerging flux tube tends to be caused by kink instability if the accumulated helicity and writhe have the same sign. Hence, we conclude that the metastable structure before eruption is a kinked flux tube.

What's the trigger mechanism for this kinked flux tube? A kinked flux tube can erupts because of kink instability. There are already some evi-

dences from observational results such as Rust & LaBonte (2005) and Liu et al. (2007, 2008) or from simulation results such as Fan (2005) and Török & Kliem (2005). Another possible trigger mechanism is the torus instability. When the confining poloidal field decreases with distance fast enough, radially outward perturbations of the flux rope could trigger the torus instability (Kliem & Török, 2006) before the helical kink instability set in, and the toroidal flux rope would no longer be confined. Fan & Gibson (2007) performed 3D simulations to investigate two distinct mechanisms that led to the eruption of the flux tube. One case (case K) is the emerging flux rope is kinked and a kink instability develops in it, leading to an eruption at last. The other one (case T) is the overlying field declines more rapidly with height, and the emerging flux rope is found to lose equilibrium and erupt via the torus instability. The corresponding normal relative magnetic helicity H_m/Φ^2 reaches approximately -0.16 for case K and approximately -0.18 for case T. However, in our observation result the normalized magnetic helicity is about -0.036 when the flux tube in AR 9729 erupted, which is one order smaller than the simulation results.

Gilbert et al. (2001) explored the various magnetic configurations for failed and partial eruptions of filaments and cavities. They suggested that reconnection at different positions of the flux rope that threads into the filament creates different topologies with implications of full, partial, or failed filament eruptions. Reconnection occurs within the prominence can cause partial filament to erupt and the rest part survive after eruption. Moore et al. (2001) also proposed a 3D Tether-Cutting model to explain the eruption process of a sigmoid structure. They conjecture that the magnetic explosion was unleashed by runaway tether-cutting via implosive/explosive reconnection in the middle of the sigmoid, as in the standard model. This internal reconnection apparently begins at the very start of the sigmoid eruption and grows in step with the explosion, caused the explosion to be ejective. In our observation, the bright point in the middle of sigmoid structure could be found clearly. Two magnetic field cancellation regions also existed before eruption and disappeared after eruption reflect the existence of reconnection there. Therefore we propose that field lines rooted to the photosphere near the inversion line where for the formation of a magnetic tangential discontinuity are locally reconnection and cause an instability. Field lines above the surface are detached from the photosphere to form this CME and partially open the field which make the filament loses equilibrium to rise quickly and then be drawn back by the tension force of magnetic field after eruption to form

a new filament in our observation.

The eruption happened when the accumulated magnetic approach near the maximum. It probably related to the possible existence of upper bounds of total relative magnetic helicity for force-free magnetic field in unbounded space, as conjectured in [Zhang et al. \(2006\)](#) on the study of axis-symmetric force-free field solutions. The absolute normalized helicity is 0.036 ± 0.054 , which is also close to the theoretical prediction value 0.035 of [Zhang et al. \(2008\)](#) when a multipolar force-free magnetic field structure could sustain before eruption.

Acknowledgements

This study is supported by grants 11078012, 11173033, 11125314, 10733020, 10921303, 41174153, 11103038 and 10673016 of National Natural Science Foundation of China, and 2011CB811400 of National Basic Research Program of China and *KLSA2010-06* of the Collaborating Research Program of National Astronomical Observatories, Chinese Academy of Sciences.

References

- Antiochos, S. K., Dahlburg, R. B., & Klimchuk, J. A., The magnetic field of solar prominences, *ApJ*, 420, L41, 1994.
- Berger, M., A. & Field, G., B., The topological properties of magnetic helicity, *J. Fluid Mech.*, 147, 133, 1984.
- Brueckner, G. E. et al., The Large Angle Spectroscopic Coronagraph (LASCO), 162, 357, 1995.
- Chae, J., Observational determination of the rate of magnetic helicity transport through the solar surface via the horizontal motion of field line foot-points, *ApJ*, 560, L95, 2001.
- Canfield, R. C., Hudson, H. S., & McKenzie, D. E., Sigmoidal morphology and eruptive solar activity, *Geophys. Res. Lett.*, 26, 627, 1999.
- Delaboudinière et al., EIT: Extreme-Ultraviolet Imaging Telescope for the SOHO Mission, *Solar Phys.*, 162, 291, 1995.

- Démoulin, P. & Berger, M. A., Magnetic Energy and Helicity Fluxes at the Photospheric Level, *Solar Phys.*, 215, 203, 2003.
- Fan, Y., Zweibel, E. G., Linton, M. G., & Fisher, G. H., The Rise of Kink-unstable Magnetic Flux Tubes and the Origin of delta-Configuration Sunspots, *ApJ*, 521, 460, 1999.
- Fan, Y., Coronal Mass Ejections as Loss of Confinement of Kinked Magnetic Flux Ropes, *ApJ*, 630, 543, 2005.
- Fan, Y. & Gibson, S. E., Onset of coronal mass ejections due to loss of confinement of coronal flux ropes, *ApJ*, 668, 1232-1245, 2007.
- Feynman, J. & Martin, S. F., The initiation of coronal mass ejections by newly emerging magnetic flux, *JGR*, 100, 3355, 1995.
- Fong, B. H., Hurricane, O. A., Cowley, S. C., Equilibrium and Stability of Prominence Flux Ropes, *Sol. Phys.*, 201, 93, 2001.
- Forbes, T. G., & Priest, E. R., Photospheric Magnetic Field Evolution and Eruptive Flares, *ApJ*, 446, 377, 2005.
- Forbes, T. G., Priest, E. R., & Isenberg, P. A., On the maximum energy release in flux-rope models of eruptive flares, *Solar phys.*, 150, 245, 1994.
- Gibson, S. E., & Fan, Y., The Partial Expulsion of a Magnetic Flux Rope, *ApJ*, 637, L65, 2006.
- Gilbert, H. R., Alexander, D., & Liu, R., Filament Kinking and Its Implications for Eruption and Re-formation, *Sol. phys.*, 245, 287, 2007.
- Gilbert, H. R., Holzer, T. E., & Burkepile, J. T., Observational Interpretation of an Active Prominence on 1999 May 1, *ApJ*, 549, 1221, 2001.
- Lin, J., Soon, W., Baliunas S. L., Theories of solar eruptions: a review, *New Astronomy Reviews*, 47, 53, 2003
- Ji, H., Wang, H., Schmahl, E. J., Moon, Y. J., & Jiang, Y., Observations of the Failed Eruption of a Filament, *ApJ*, 595, L135, 2003.
- Kliem, B., & Török, T., Torus Instability, *Ph. Rv. Lett.* 96, 5002, 2006.

- Leamon, R. J., Canfield, R. C., Blehm, Z., Pevtsov, A. A., What Is the Role of the Kink Instability in Solar Coronal Eruptions?, *ApJ*, 596, 255L, 2003.
- Leka, K. D., Canfield, R. C., McClymont, A. N., & van Driel-Gesztelyi, L., Evidence for Current-carrying Emerging Flux, *ApJ*, 462, 547, 1996.
- Leka, K. D., Fan, Y., Barnes, G., On the Availability of Sufficient Twist in Solar Active Regions to Trigger the Kink Instability, *ApJ*, 626, 1091L, 2005.
- Linton, M. G., Dahlburg, R. B., Fisher, G. H., & Longcope, D. W., Nonlinear Evolution of Kink-unstable Magnetic Flux Tubes and Solar delta-Spot Active Regions, *ApJ*, 507, 404, 1998.
- Liu, J. & Zhang, H., The magnetic field, horizontal motion and helicity in a fast emerging flux region which eventually forms a delta spot, *solar physics*, 234, 21, 2006.
- Liu, R., Alexander, D., & Gilbert, H. R., Kink-induced Catastrophe in a Coronal Eruption, *ApJ*, 661, 1260, 2007.
- Liu, R., Gilbert, H. R., Alexander, D., & Su, Y., The Effect of Magnetic Reconnection and Writhing in a Partial Filament Eruption, *ApJ*, 680, 1508, 2008.
- Lopez Fuentes, M. C., Démoulin, P., Mandrini, C. H., & Pevtsov, A. A., Magnetic twist and writhe of active regions. On the origin of deformed flux tubes, *Astron. Astrophys.*, 397, 305, 2003.
- Low, B. C., Coronal mass ejections, magnetic flux ropes, and solar magnetism, *J. Geophys. Res.*, 106, A11, 25, 141, 2001.
- Low, B. C., & Zhang, M., The Hydromagnetic Origin of the Two Dynamical Types of Solar Coronal Mass Ejections, *ApJ*, 564, 53L, 2002.
- Mikic, Z. & Linker, J. A., Disruption of coronal magnetic field arcades, *ApJ*, 430, 898, 1994.
- Moore, R. L., Sterling, A. C., Hudson, H. S. ,& Lemen, J. R., Onset of the magnetic explosion in solar flares and coronal mass ejections, 552, 833-848, 2001.

- Rust, D. M., & Kumar, A., Evidence for Helically Kinked Magnetic Flux Ropes in Solar Eruptions, *ApJ*, 464, L199, 1996.
- Rust, D. M., & LaBonte, B. J., Observational Evidence of the Kink Instability in Solar Filament Eruptions and Sigmoids, *ApJ*, 622, L69, 2005.
- Romano, P., Pariat, E., Sicari, M., & Zuccarello, F., A solar eruption triggered by the interaction between two magnetic flux systems with opposite magnetic helicity, *A&A*, 525, A13, 2011
- Pariat, E., Démoulin, P., & Berger, M. A., Photospheric flux density of magnetic helicity, *A&A*, 439, 1191, 2005
- Priest, E. R., & Forbes, T. G., The evolution of coronal magnetic fields, *Solar phys.*, 130, 399, 1990.
- Priest, E. R., & Forbes, T. G., The magnetic nature of solar flares, *A&A Rev.*, 10, 313, 2002.
- Schmieder, B., Démoulin, P., Pariat, E., et al., Actors of the main activity in large complex centres during the 23 solar cycle maximum, *Adv. Space Res.*, 47, 2081, 2011.
- Scherrer, P. H., et al., The Solar Oscillations Investigation - Michelson Doppler Imager, *Sol. Phys.*, 162, 129, 1995
- Sturrock, P. A., Weber, M., Wheatland, M. S., & Wolfson, R., Metastable Magnetic Configurations and Their Significance for Solar Eruptive Events, *ApJ*, 548, 492, 2001.
- St. Cyr, O. C. et al., Properties of coronal mass ejections: SOHO LASCO observations from January 1996 to June 1998, *JGR*, 105, 18169, 2000.
- Török, T., & Kliem, B., Confined and Ejective Eruptions of Kink-unstable Flux Ropes, *ApJ*, 630, L97, 2005.
- Titov, V. S., & Démoulin, P., Basic topology of twisted magnetic configurations in solar flares, *A&A*, 351, 707, 1999.
- Tsuneta, S. et al., The Soft X-ray Telescope for the SOLAR-A Mission, *Sol. Phys.*, 136, 37, 1991.

- Weart, S. R., The Birth and Growth of Sunspot Regions, *ApJ*, 162, 987, 1970.
- Weart, S. R., What Makes Active Regions Grow?, *ApJ*, 177, 271, 1972.
- Welsch, B.T., Abbett, W.P., De Rosa, M.L., et al., Tests and Comparisons of Velocity-Inversion Techniques, *ApJ*, 670, 1434, 2007.
- Williams, D. R., Török, T., Démoulin, P., vanDriel-Gesztelyi, L., & Kliem, B., Eruption of a Kink-unstable Filament in NOAA Active Region 10696, *ApJ*, 628, L163, 2005.
- Yang, S., Büchner, J. & Zhang, H., Magnetic helicity exchange between neighboring active regions, *ApJ*, 695, L25, 2009a.
- Yang, S., Zhang, H., & Büchner, J., Magnetic helicity accumulation and tilt angle evolution of newly emerging active regions, *A&A*, 502, 333, 2009b.
- Zhang, M., Flyer, M., & Low, B., Magnetic Field Confinement in the Corona: The Role of Magnetic Helicity Accumulation, *ApJ*, 644, 575., 2006.
- Zhang, M., & Flyer, N., The Dependence of the Helicity Bound of Force-Free Magnetic Fields on Boundary Conditions, *ApJ*, 683, 1160, 2008.

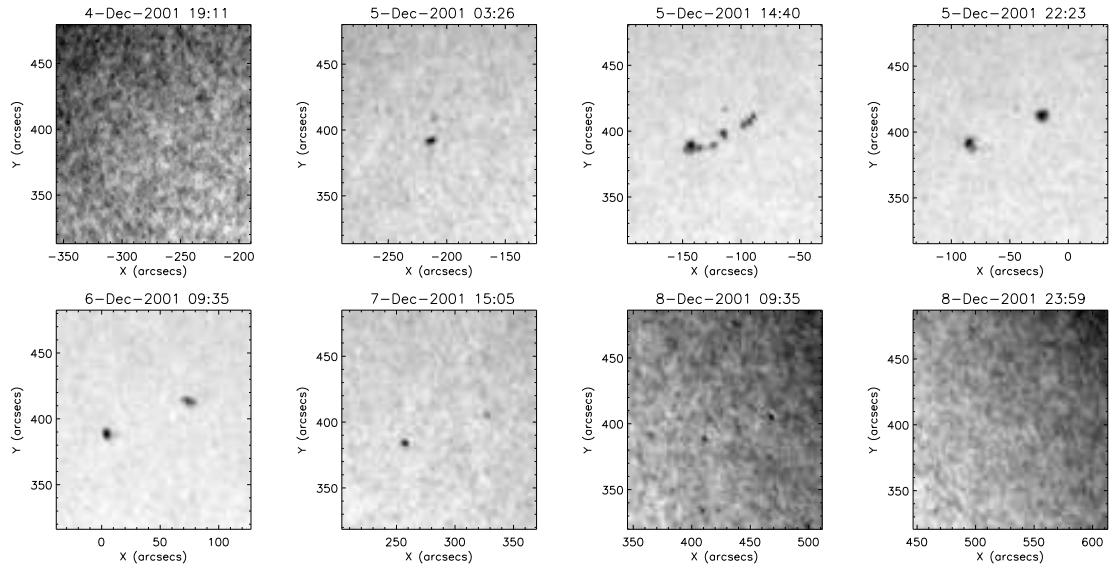


Figure 2: WL evolution.

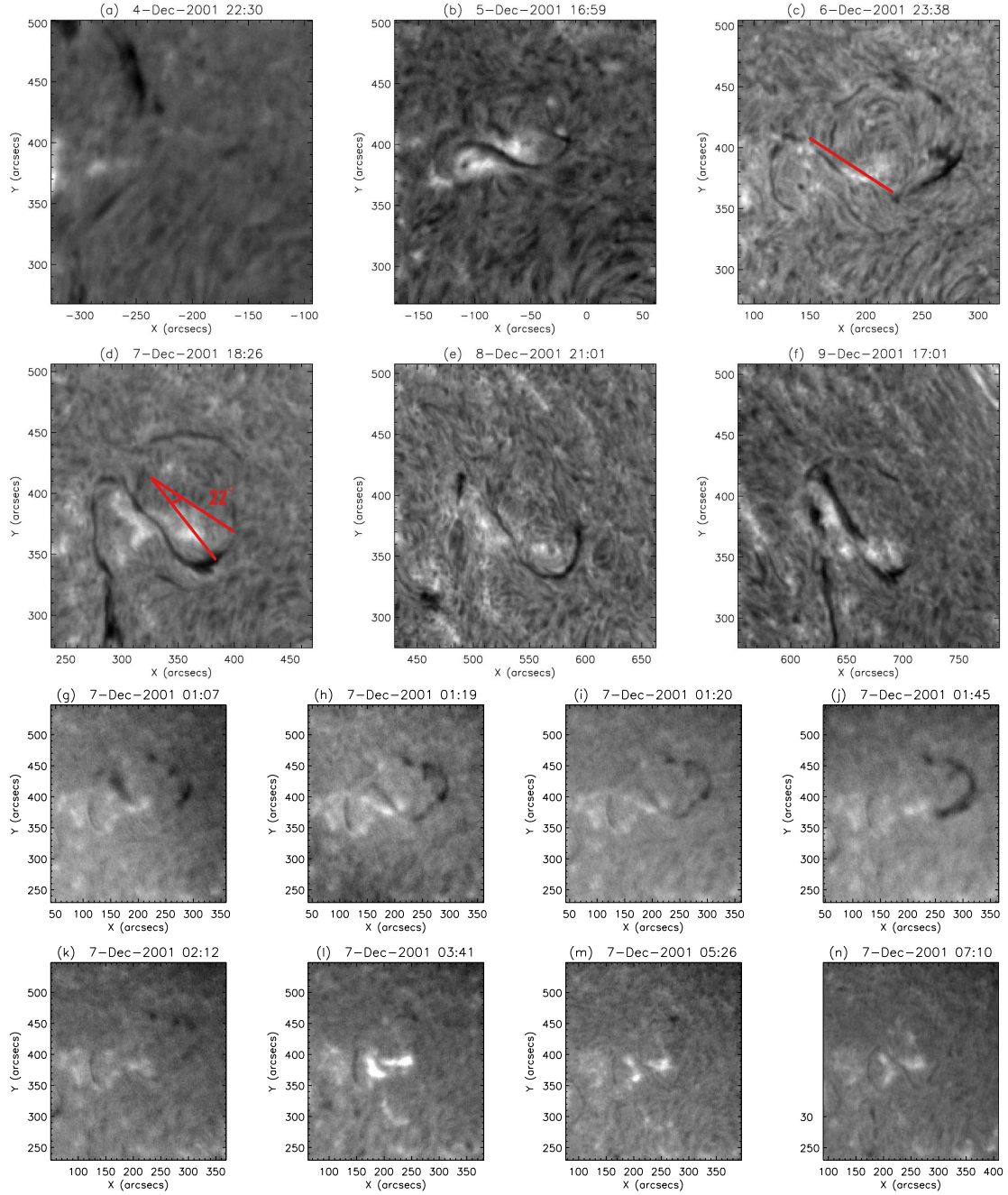


Figure 3: Time Sequence of $H\alpha$ images. Top two rows show the evolution of $H\alpha$ from December 04 to 09, 2001. Bottom two rows show the evolution of $H\alpha$ in the filament eruption on December 07.

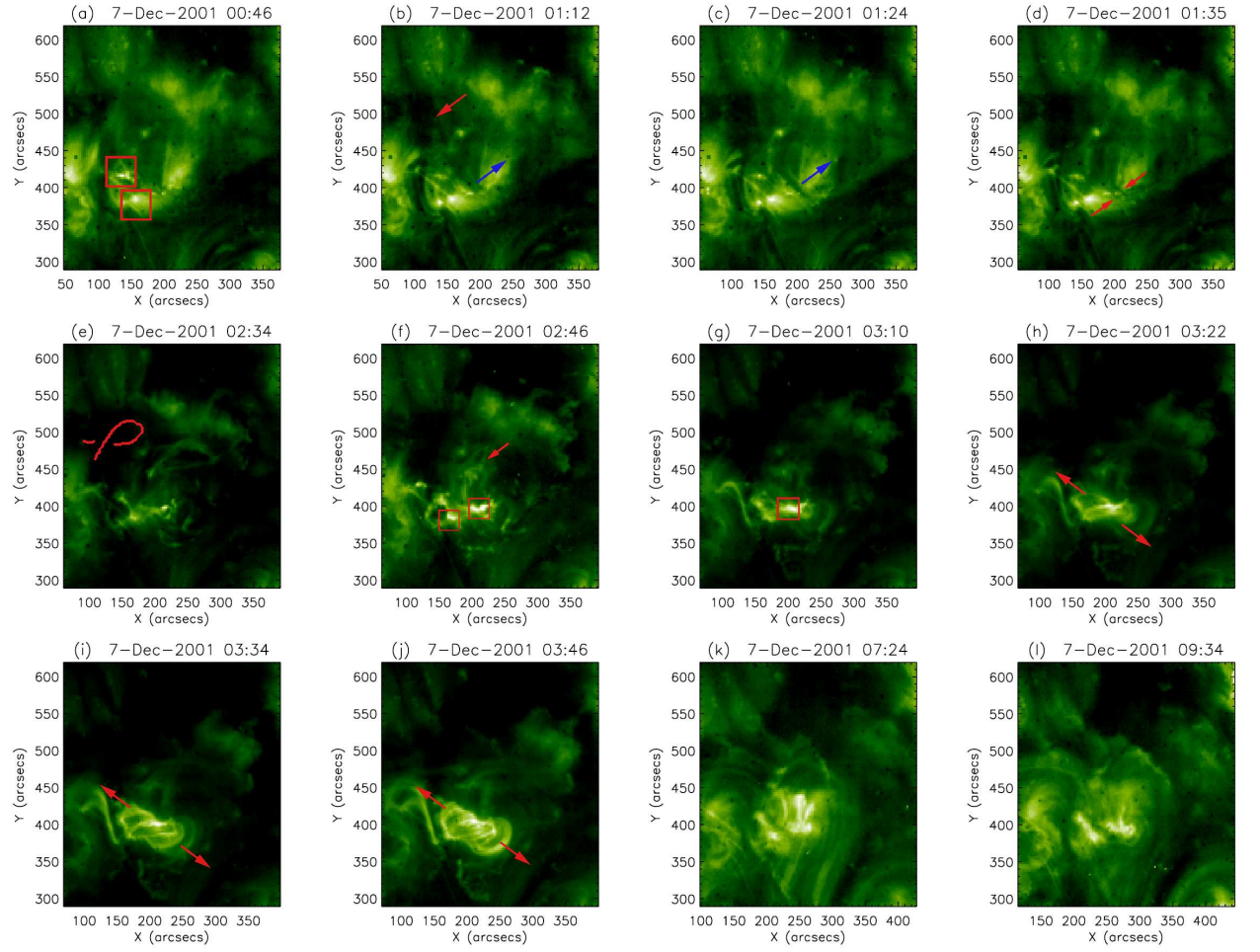


Figure 4: EIT evolution in the eruption on December 07,2001.

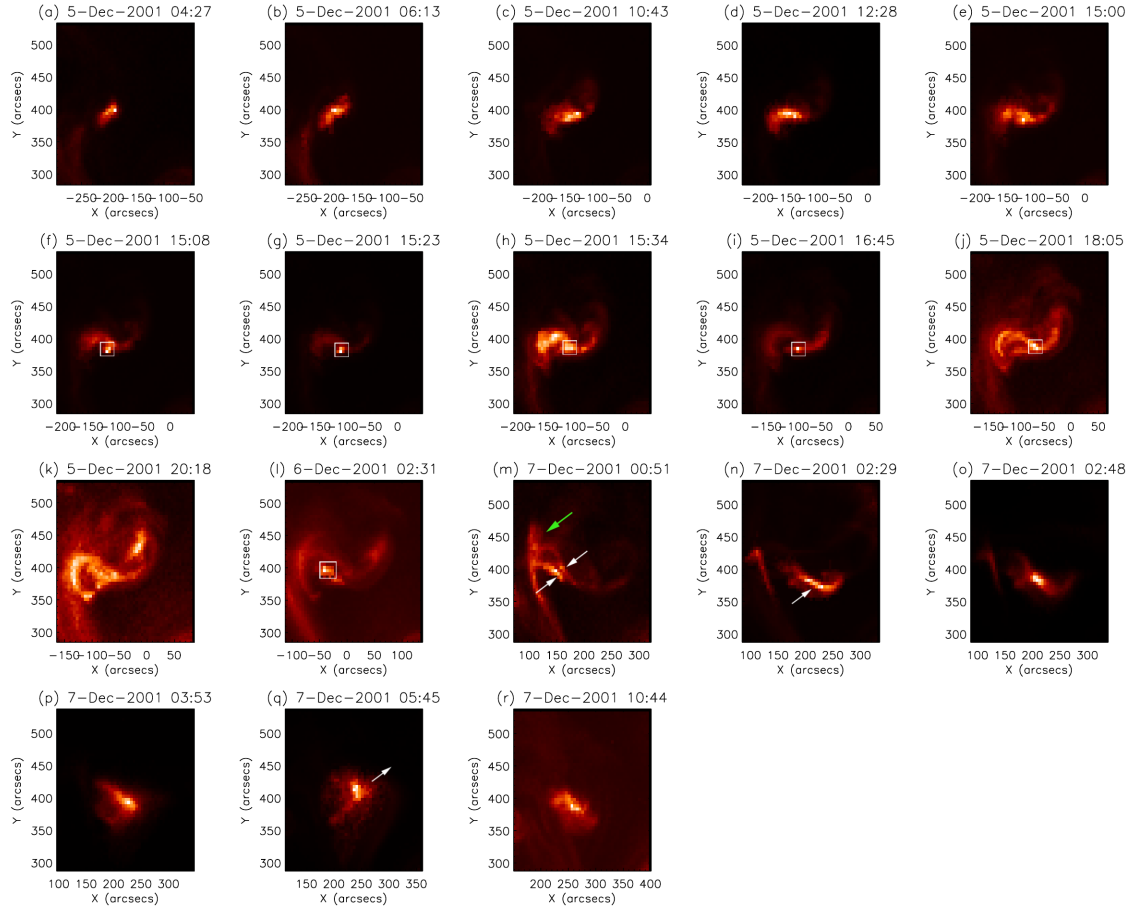


Figure 5: Time Sequence of Yohkoh SXT images.

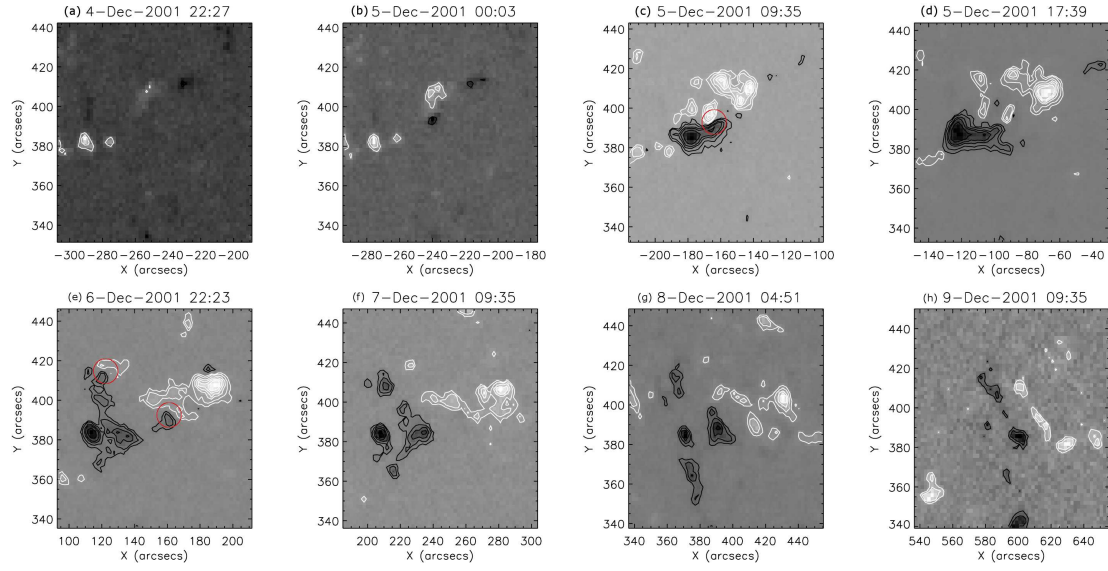


Figure 6: Evolution of line-of-sight magnetic field from November 04 to 09, 2001. Positive (negative) magnetic flux is indicated by white (black) solid lines at 100, 200, 400, 600 and 1000 G.

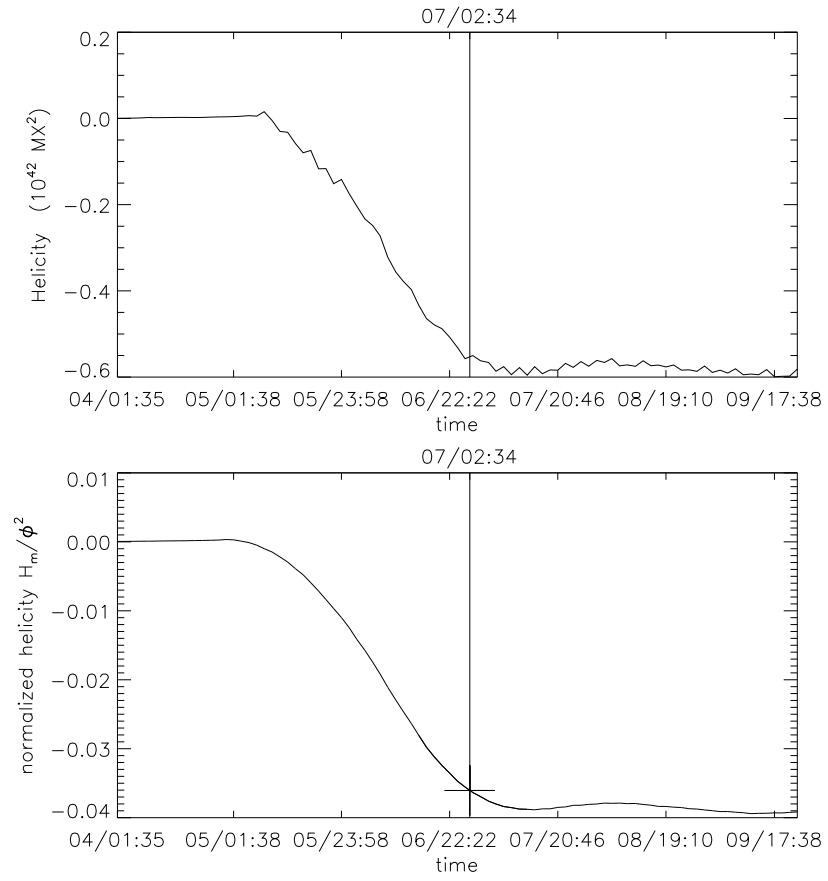


Figure 7: The time profile of normalized parameter for NOAA 9729.

